to investigate the effect of temperature dependent optical properties on the solutions assuming that the influence of temperature on the properties themselves can be found. Similarly the effects of the variation of thermal and strength properties with temperature should be examined.

Finally, the transpiration or sublimation effects were applied at the exposed surface, and it would be useful to fully blend these into the differential equation to get a more accurate picture of how they influence material response deep within the coating.

References

[1] Howe, J. T., "Shielding of Partially Reflecting Stagnation Surfaces Against Radiation by Transpiration of an Absorbing Gas," TR-R-95, 1961, NASA.

[2] Allen, H. J., "Gas Dynamics Problems of Space Vehicles," *Gas Dynamics in Space Exploration*, NASA SP-24, 1962.

[3] "Optical Crystals," Bulletin 1100, Isonet Corp., Palisades Park, N.J., 1963, p. 36.

[4] Love, T. J., *"Radiative Heat Transfer,"* Charles E. Merrill, Columbus, Ohio, 1968, p. 220.

[5] Nachtsheim, P. R., Peterson, D. L., and Howe, J. T., "Reflecting Ablative Heat Shields for Radiative Environments," Paper AAS-71-147, 1971, AAS.

[6] Peterson, D. L., Nachtsheim, P. R., and Howe, J. T., "Reflecting Ablating Heat Shields for Planetary Entries," AIAA Paper 72-89, San Diego, Calif., 1972.

[7] Howe, John T., "Thermal-Mechanical Response of Nearly Opaque Materials Exposed to Continuous Radiation," *AIAA Journal*, Vol. 9, No. 10, Oct. 1971, pp. 1911–1920.

[8] Penner, S. S. and Sharma, O. P., "Interaction of Laser Radiation with an Absorbing Semi-Infinite Solid Bar," *Journal of Applied Physics*, Vol. 37, No. 6, 1966, p. 2304.

[9] Timioshenko, S. P. and Goodier, J. N., *Theory of Elasticity*, McGraw-Hill, New York, 1951, p. 420.

[10] Weston, K. C., Howe, J. T., and Green, M. J., "Approximate Temperature Distribution for a Diffuse, Highly Reflecting Material," *AIAA Journal*, Vol. 10, No. 9, Sept. 1972, pp. 1252–1254.

[11] Shepard, C. E., "Advanced High Power Arc Heaters for Simulating Entries into the Atmospheres of the Outer Planets," AIAA Paper 71-263, Albuquerque, N. Mex., 1971.

JANUARY 1973 AIAA JOURNAL VOL. 11, NO. 1

Raman Scattering from Pollutant Gases and Air-Water Interfaces

RONALD L. SCHWIESOW*

Environmental Research Laboratories, National Oceanic and Atmospheric Administration, Boulder, Colo.

Remote sensing of environmental constituents by Raman lidar is an attractive method for monitoring molecular environmental pollutants. We report techniques for and results of laboratory measurements of Raman scattering cross sections and depolarization ratios of atmospheric gases, as a function of incident photon energy. The cross section of H_2O (relative to N_2 as a reference) changes by a factor of 2 as the incident photon energy is changed by 5%. Results for SO_2, NO, and other gases are less dramatic. We also discuss preliminary spectral features of scattering from polluted air-water interfaces.

I. Applications of Spectral Back-Scatter

RAMAN lidar involves the spectral and temporal resolution of the optical back-scatter of a monochromatic pulsed laser source. The intensity-vs-photon-energy characteristics of the scattered spectrum for a given laser photon energy (or frequency) identify the scatterer, and the time delay determines range to the scatterer. In principle, such an atmospheric or air-to-water interface scattering technique is a powerful remote sensor for environmental pollutants.

Our laboratory is involved in studies of the Raman scattering characteristics of gases, aerosols, and air-to-liquid interfaces. The purpose of this paper is to identify some illustrative applications of generalized Raman scatter to pollutant systems, and then to discuss in this applications context, some preliminary results of our laboratory measurements. The paper is designed to serve as a review of applications and theory and as a preview of scattering results.

Enthusiasm for the ability of Raman lidar to both identify and locate a particular polluting constituent must be tempered by the fact that gaseous Raman scattering is very weak compared to Mie or Rayleigh scattering. Scattering cross section and depolarization ratio are the two quantitative parameters which describe the magnitude of the molecular Raman scattering interaction. These parameters will be described in more detail later. Together with the incident laser frequency and the characteristic frequency shift of the particular molecular transition, the cross section and depolarization ratio completely describe the scattering interaction. These four characteristic scattering values, over a range of the incident laser photon frequency as an independent variable, must be known for molecules of interest in order to make realistic system feasibility studies, to calibrate field sensor equipment, and to select laser frequencies for maximum back-scatter intensity. These molecular measurements are discussed here. Similar laboratory studies of gaseous scattering from different molecules from those discussed in this paper have recently been reported by Widhopf and Lederman.[1]

Although many investigators have proposed Raman lidar measurements of atmospheric pollutants, Kobayasi and Inaba[2]

Presented as Paper 71-1086 at the Joint Conference on Sensing of Environmental Pollutants, Palo Alto, Calif., November 8–10, 1971; submitted October 28, 1971; revision received July 31, 1972. Research supported in part by NASA, MSC and EPA, APCO.

Index categories: Atmospheric, Space, and Oceanographic Sciences; Lasers.

* Physicist.

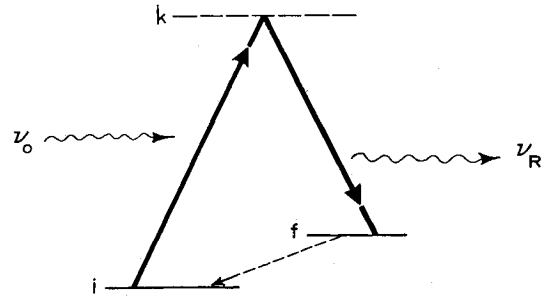

Fig. 1 Representative energy level diagram for discussing the Raman effect.

are among the few to report positive results. Optimization and interpretation of such results require quantitative molecular studies.

We suggest that Raman lidar may also be a useful tool for water pollution studies. Pollution analysis by bulk Raman scattering from samples in small cells has been suggested and demonstrated to a limited extent.[3] This paper reports preliminary spectra of Raman scattering from air-to-water interfaces. This method of characterizing water-borne pollutants is excellently suited to remote sensing of large areas from an air-borne platform. Lidar has considerably more flexibility than other methods, such as solar uv absorption, because the active, controlled source allows rapid scanning, ratio detection, and selection of monochromatic pump frequency. One can visualize a remote sensing method utilizing a lateral scan from an aircraft coupled with translation along the aircraft track.

Remote analysis of pollutant systems by Raman back-scatter is currently signal-to-noise limited by technological problems (laser power and optical filter bandwidth) and by lack of understanding of the details of molecular scattering. Advantages of the remote methods over point sampling, including speed, economy and large area coverage, dictate that research on these questions continue.

II. The Raman Effect

At least three types of spectrally-dependent processes are useful for remote constituent sensing. They are resonance reradiation, fluorescence, and Raman scattering. At atmospheric pressures only Raman scattering has been observed for molecules, so we will emphasize the Raman effect in the following discussion. Qualitative aspects of the scattering are also useful for understanding resonance reradiation and fluorescence effects.

The energy level diagram useful for reviewing the Raman effect is shown in Fig. 1. For molecular pollutants, vibration-rotation levels are applicable, although the theory[4] applies to pure rotation and electronic energy levels, as well as more complex energy states in solids and liquids. For Raman scattering the level k is a virtual (or unreal) state of the molecule. Level k is introduced as a conceptual aid in visualizing the interaction in terms of energy conservation. The scattering involves the interaction of a molecule and two photons simultaneously, and

$$\sigma(\nu) \propto (\nu_o + \nu_{if})^4 P_{if}^2$$

$$P_{if} = \frac{1}{h} \sum_k \frac{\langle \psi_i | \bar{r} | \psi_k \rangle \langle \psi_k | \bar{r} | \psi_f \rangle}{\nu_{ki} - \nu_o + i\delta_k} + \frac{\langle \psi_f | \bar{r} | \psi_k \rangle \langle \psi_k | \bar{r} | \psi_i \rangle}{\nu_{kf} + \nu_o + i\delta_k}$$

Fig. 2 Quantum mechanical expression for the differential Raman scattering cross section of a gaseous molecule.

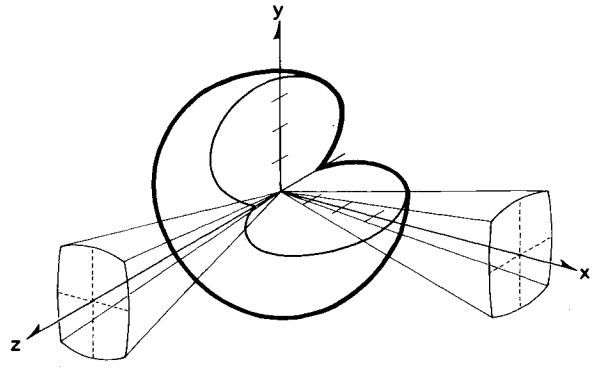

Fig. 3 Representative three-dimensional Raman scattering diagram for scattering intensity as a function of angle. Laser radiation is directed along the y axis polarized in the z direction. Instrumental collection solid angles are indicated for viewing scattering in the x and z directions.

is referred to as a single two-photon interaction. In this context, simultaneously means a time less than 10^{-16} sec. Energy is conserved in the over-all process, but is not conserved in the individual photon destruction and creation subprocesses, where all real states of the molecule are involved. Since the two-photon scattering occurs so rapidly, it is not affected by molecular collisions which typically involve mean time between collisions of the order of 10^{-8} sec.

If state $i \equiv$ state f but k still represents a virtual state, the energy level diagram applies to Rayleigh scattering. This type of scattering is also a two-photon interaction with the molecule, but there is no measurable difference in the incident and scattered photon energies. When k is a real state of the molecule, then the energy level diagram applies to fluorescence if state $i \neq$ state f, and to resonance reradiation if state $i \equiv$ state f. Fluorescence and resonance reradiation involve two separate interactions of the molecule with a single photon at a time. This is referred to as a sequence of two single-photon interactions. The time lapse between stages of the process varies widely but is typically 10^{-6} sec. Energy is conserved in each step of the process. The time lapse between the two single-photon interactions with the molecule allows molecular collisions to nonradiatively de-excite the molecule, quenching the fluorescence or reradiation.

The expression[5] governing Raman scattering intensity is shown in Fig. 2. The incident photon frequency is ν_o, and the double subscript frequency $\nu_{if} = \nu_i - \nu_f$ denotes a frequency difference which is proportional to an energy level difference in the molecule. The matrix elements are summed over all real states k of the molecule. The resonance damping factor δ_k may be different for each real state, and is related to the uncertainty or width of the energy level. The equation shows scattering cross-section variation with incident (pump) frequency ν_o. Since the wave functions ψ are not known for molecules of interest, the expression is not useful for calculation of cross sections directly; laboratory measurements are required. The expression demonstrates the "ν^4 law" characteristic of Raman and Rayleigh scattering alike. This means the scattering cross section is relatively much larger for higher energy incident photons. The resonance denominators are demonstrated and quantified in the next section. Resonance Raman scattering is predicted when the incident frequency is nearly the same as the difference between a real intermediate state and either the initial or final states.[4] The magnitude of the cross-section change caused by the resonance denominator is the order of 10^6 for some organic liquids.[5]

III. Gaseous Cross Section Studies

Method

In order to measure molecular scattering characteristics, we conduct carefully controlled laboratory experiments. The equip-

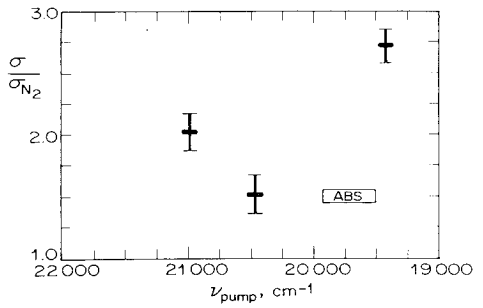

Fig. 4 Relative Reman scattering cross section for water vapor under atmospheric conditions and various laser pump photon energies. A region of weak water vapor absorption is indicated schematically as ABS (the ordinate of the region has no significance) for comparison with Fig. 2.

ment includes a CW argon-ion laser, double monochromator to discriminate against instrumentally scattered on-frequency light and a linear photon-counting detection scheme. All data are taken and processed using digital techniques.

The three-dimensional molecular scattering pattern of a fluid is indicated in Fig. 3, relating intensity and angle. The minimum and maximum radial dimensions of the toroid characterize the scattering and give the cross section and depolarization ratio for the scattering process at some particular pump frequency and molecular frequency shift. The scattering cross section is the magnitude of the maximum radial dimension of the toroid, while the depolarization ratio is the ratio of minimum to maximum dimensions. This depolarization ratio is the same as that obtained by measuring the ratio of y to z polarized scattering for light propagating in the x direction. Because the scattered photons are collected over a large solid angle, the minimum and maximum intensities of Fig. 3 are not available directly, but are obtained from geometrical corrections. Similar corrections are required for the polarization sensitivity of the monochromator.

Pollutant gases are measured in a cell buffered with nitrogen to 760-torr total pressure. The nitrogen reproduces atmospheric pressure-quenching effects and serves as an internal intensity reference. Reported cross sections are given relative to the integrated scattering of the single, isolated Q branch of nitrogen at a shift ν_{if} of 2331 cm^{-1} from the exciting light. In the region of incident photon energy 10,000–40,000 cm^{-1}, nitrogen has no known absorptions and is presumed to exhibit only the $(\nu_o + \nu_{if})^4$ frequency dependence.

Four argon laser lines have sufficient power to yield significant scattered intensity for useful measurements on gases.

Results

The results reported must be applied with care since further measurements may refine these values. General characteristics of the variation in cross section with pump frequency are believed correct and useful.

Figure 4 graphically illustrates the variation in the Raman scattering cross section of water vapor with incident photon energy. The very weak visible absorption indicated schematically is probably the reason for the weak cross-section resonance. Studies with a tunable dye laser closer to the absorption region are in process, and should help us understand the intensity equation.

The table of scattering cross sections (Table 1) summarizes results to date on pollutant molecules. The values are consistent with other measurements[6–8] which were not polarization-analyzed. Larger cross sections are required to extend the range or pollutant concentration limits of present systems.[2] Resonance studies hold promise of selecting optimum laser frequencies for this extension. Depolarization measurements are an important part of understanding the resonance denominators.[4]

An excitingly large cross section for mixed hydrocarbon vapors is indicated in Fig. 5. This data has not yet been analyzed for cross section, but on the basis of relative integrated spectral areas and sample partial pressures, it appears that the average hydrocarbon cross section is approximately 115 times that of nitrogen. The spectrum is the result of the C—H stretch in the molecules, where the energy shift for each bond depends on the host molecule and bond location. This molecular combination results in a broad spectrum compared to the nitrogen spectrum. Further analysis of this pollutant system is important for remote sensing purposes.

Table 1 Measured relative Raman cross sections ($\sigma_{N_2} = 1$)

Gas	Laser wave number, cm^{-1}	Relative cross section	Depolarization
SO_2	20 981 (476.5nm)	5.2	0.04
	20 487 (488.0nm)	5.5	0.05
	20 135 (496.5nm)	5.5	0.04
	19 430 (514.5nm)	5.6	0.05
NO	20 981	0.45	0.11
	20 487	0.45	0.10
	20 135	0.43	0.11
	19 430	0.49	0.08
H_2O	20 981	2.5	
	20 487	1.9	
	19 430	3.3	

IV. Air-Liquid Interface Studies

Raman scattering in liquids is comparatively more intense than scattering in gases. An air-liquid interface scatters with a spectrum very similar to that of the bulk liquid. Based on results discussed in this section, Raman (or fluorescent) scattering is a useful analytical tool in water pollution studies.

The apparatus for laboratory studies is basically the same as that described for gaseous measurements. Samples are contained in quartz tubes for 90° bulk scattering, or the air-water interface is illuminated and examined at near-normal incidence. The latter sampling method more realistically models the situation involved in remote sensing. A deep cell is used for interface measurements so that the transmitted beam is removed from the scattering region.

Remote measurements of water temperature are possible using the Raman effect. Such remote temperature measurements are valuable for a study of thermal water pollution using the sensing techniques outlined in Sec. I. Scattering is independent of the surface emissivity and intervening atmospheric temperature.

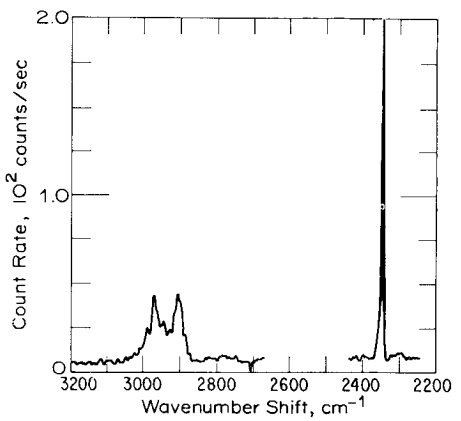

Fig. 5 Raman scattering spectrum of mixed hydrocarbons in gasoline vapor. Nitrogen reference is at a shift of 2331 cm^{-1} with the hydrocarbon spectrum in the region of 2850–3050 cm^{-1} shift. Data not corrected for instrumental response.

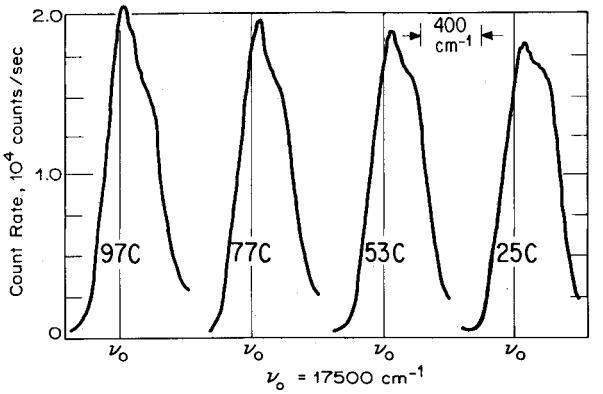

Fig. 6 Raman scattering spectrum of synthetic sea water at four different temperatures. Laser pump at 20487 cm^{-1}. ν_o indicates photon frequency fiducial point for comparison of spectra.

These latter two parameters affect infrared radiometer measurements of water temperature. Raman spectra of the principal liquid water peak in a synthetic ocean water sample as a function of temperature are shown in Fig. 6. These results are similar to measurements in pure water made by Walrafen.[9] A significant observation is that the presence of ionic solutes in the water does not change the temperature dependence of the spectrum. By measuring the ratio of scattered intensity at the two peaks (or at one shoulder and the isosbestic[8] point near 3460 cm^{-1} shift), one has a self-calibrating determination of water temperature. This can be measured at the same time that other pollutant aspects are measured by scattering, as discussed below. These spectra were taken in bulk samples (volume scattering), as were Walrafen's, but one expects identical results from interface scattering.

To detect trace constituents by Raman scattering, one must suppress the liquid water spectrum. In very recent data, taken digitally, we have subtracted point-by-point the pure water spectrum from the polluted water spectrum. Such difference spectra have been run on samples of water from the Miami, Florida and Washington, D. C. areas. These samples were provided by the National Ocean Survey. The analysis has progressed only far enough to say that there are significant differences in the samples in broadband features and in a few sharp spectral features. For example, a spectral peak is associated with ocean

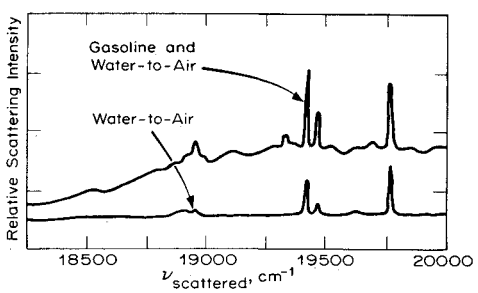

Fig. 7 Raman spectrum of an air to gasoline on water interface. Laser pump at 20487 cm^{-1}. Air-to-pure-water interface scattering shown for comparison.

samples but not with upper-river or NaCl solution samples. More research is required on controlled samples, but the potential for remote sensing of actual water pollution is demonstrated.

Interface scattering from air to pure water and from air to gasoline on water interfaces is sketched in Fig. 7. Details of the spectrum are not yet analyzed. An obvious conclusion is that there is a significant difference in the spectra. The broadband increase and some of the enhanced spectral peaks in the gasoline-on-water spectrum are most likely instrumental scattering and grating ghost effects associated with the increased on-frequency particulate scattering of the polluted interface. Other spectral features of the upper spectrum are due to the presence of the gasoline film on the water.

V. Conclusions

Raman lidar is a potentially useful tool for remote sensing of atmospheric and water-borne pollution distributions—at least in near-source concentrations.

Our laboratory studies of pollutant systems have provided quantitative cross sections for some gaseous pollutants, and have demonstrated that significant changes in cross section occur with small changes in pump frequency. Proper selection of laser pump is important to optimize Raman lidar systems.

Studies of chemically and thermally polluted air-water interfaces have demonstrated the feasibility of mapping water-pollutant distributions by Raman lidar. Detailed analysis of the spectra is yet required to evaluate the practicality of the schemes.

References

[1] Widhopf, G. F. and Lederman, S., "Specie Concentration Measurements Utilizing Raman Scattering of a Laser Beam," *AIAA Journal*, Vol. 9, No. 2, Feb. 1971, pp. 309–316.

[2] Kobayasi, T. and Inaba, H., "Spectroscopic Detection of SO_2 and CO_2 Molecules in Polluted Atmosphere by Laser-Raman Radar Technique," *Applied Physics Letters*, Vol. 17, No. 4, Aug. 1970, pp. 139–141; "Laser-Raman Radar for Air Pollution Probe," *Proceedings of the IEEE*, Vol. 58, No. 10, Oct. 1970, pp. 1568–1571.

[3] Bradley, E. B. and Frenzel, C. A., "On the Exploitation of Laser Raman Spectroscopy for Detection and Identification of Molecular Water Pollutants," *Water Research*, Vol. 4, No. 1, Jan. 1970, pp. 125–128.

[4] Placzek, G., "Rayleigh-Streuung and Raman-Effekt," *Handbuch der Radiologie*, Vol. 6, edited by E. Marx, Akademische Verlagsgesellschaft, Leipzig, Germany, 1934, pp. 209–374; UCRL Translation No. 526 (L) by A. Werbin.

[5] Behringer, J., "Observed Resonance Raman Spectra," *Raman Spectroscopy*, edited by H. A. Szymanski, Plenum Press, New York, 1967, pp. 168–223.

[6] Leonard, D. A., "Measurement of NO and SO_2 Raman-Scattering Cross Sections," *Journal of Applied Physics*, Vol. 41, No. 10, Sept. 1970, pp. 4238–4239.

[7] Fouche, D. G. and Chang, R. K., "Relative Raman Cross Section for N_2, O_2, CO, CO_2, SO_2, and H_2S," *Applied Physics Letters*, Vol. 18, No. 12, June 1971, pp. 579–580; "Relative Raman Cross Section for O_3, CH_4, C_3H_8, NO, N_2O, and H_2," *Applied Physics Letters*, Vol. 20, No. 7, April 1972, pp. 256–257.

[8] Penney, C. M., Goldman, L. M., and Lapp, M., "Raman Scattering Cross Sections," *Nature Physical Science*, Vol. 235, No. 58, Feb. 1972, pp. 256–257.

[9] Walrafen, G. E., "Raman Spectral Studies of the Effects of Temperature on Water Structure," *The Journal of Chemical Physics*, Vol. 47, No. 1, July 1967, pp. 114–126.